Stereomicroscopic optical method for the assessment of load transfer patterns across the wood-adhesive bond interphase

Citation	Schwarzkopf, M., & Muszyński, L. (2015). Stereomicroscopic optical method for the assessment of load transfer patterns across the wood-adhesive bond interphase. Holzforschung, 69(5), 653-660. doi:10.1515/hf-2014-0098
DOI	10.1515/hf-2014-0098
Publisher	De Gruyter
Version	Version of Record
Terms of Use	http://cdss.library.oregonstate.edu/sa-termsofuse

Matthew Schwarzkopf* and Lech Muszyński

Stereomicroscopic optical method for the assessment of load transfer patterns across the wood-adhesive bond interphase

Abstract: The mechanical performance of wood-based composites is determined by the mechanical properties of their individual components and the effective load transfer between these components. In laminated wood composites, this load transfer is facilitated by the adhesive bond. The experimental methodology developed in this study measures and analyzes the full-field deformation and strain distributions across the loaded wood-adhesive interphase at a micromechanical level. Optical measurements were performed based on the principles of digital image correlation by a stereomicroscopic camera system. This system allows the monitoring of in-plane deformations as well as out-of-plane displacements, providing full-field 3D surface strain maps across the adhesive bond. These measurements can be used to improve the understanding of the load transfer between the adherents and the contribution of the adhesive to the mechanical properties of the bulk composite and serve as a quantitative input for numerical modeling and simulations aimed at the improvement of the products.

Keywords: adhesive interphase, digital image correlation (DIC), load transfer, micromechanics, optical measurement

DOI 10.1515/hf-2014-0098
Received March 28, 2014; accepted October 29, 2014; previously published online December 17, 2014

Introduction

The mechanical performance of adhesive-bonded wood-based composites is determined by the mechanical properties of their individual components and the internal bonds providing effective load transfer between these components. During manufacture, the prepolymeric liquid adhesive penetrates the cell structure of the wood adjacent to the bond. This penetration is commonly observed on the cell lumen level, although there is evidence that some adhesive systems penetrate the submicron pore system in the cell wall (Kamke and Lee 2007). This region is commonly referred to as the interphase and is defined by Kamke et al. (2014) as "the bond consisting of cell wall substance, voids, and voids filled with adhesive".

The performance of the wood-adhesive system may be modified to some extent by changing the composition and the internal structure of the bond by adjusting the resin viscosity, resin spread rates, and bonding pressures. The ability to reliably correlate these parameters with bond performance and bulk properties of the composite are critical for predicting the effect of the modifications, modeling, and virtual prototyping of innovative and more efficient adhesive systems (Kamke et al. 2014).

However, the precise measurement of the effects of such modification depends on a reliable quantitative assessment of the efficiency of the load transfer across adhesive bond interphases at the micrometer level. It is fair to say that up-to-date reliable measurement of the micromechanical interactions in complex, heterogeneous media at a micrometer scale remains a major challenge.

Standard test methods check the overall effect of such modifications in bulk composites. Shear tests are frequently used in this context: the shear plane is focused on the bondline so that the load is transferred through the wood pieces either by compression (ASTM D2339-98, 2011; ASTM D906-98, 2011; ASTM D905-08, 2013) or by tension (ASTM D2339-98, 2011; ASTM D906-98, 2011). These tests are conventional quality-control tools where the standard pass/fail criterion is based on the combined information about the failure mode (wood fracture fraction) and the ultimate failure load of the specimen. However, they do not provide well-defined material characteristics and cannot address the bond performance in the context of its complex 3D microstructure.

***Corresponding author: Matthew Schwarzkopf,** Department of Wood Science and Engineering, Oregon State University, 119 Richardson Hall, Corvallis, OR 97331, USA,
e-mail: matthew.schwarzkopf@oregonstate.edu
Lech Muszyński: Department of Wood Science and Engineering, Oregon State University, 119 Richardson Hall, Corvallis, OR 97331, USA

At the micrometer scale, Müller et al. (2005) and Serrano and Enquist (2005) optically measured displacements and strains on adhesively bonded wood laminate specimens prepared for the standard test methods EN 302-1 and ASTM D905 using electronic speckle pattern interferometry (ESPI) and digital image correlation (DIC). A comparison of the two methods by Valla et al. (2011) revealed that both are suitable for the analysis of displacement and strain distribution of wood composites. Serrano and Enquist (2005) observed areas of approximately 20×20 mm^2 (EN 302-1) and approximately 30×60 mm^2 (ASTM D905) with a reported displacement resolution of ±0.1 mm. Müller et al. (2005) observed an area of 20×15 mm^2 and reported the ESPI method being capable of ±0.05 µm. Both studies used techniques with microlevel resolution, but the analyses were of the macrobondline area and not at a scale accounting for specimen-specific micromorphology.

At the submicron scale, Clauß et al. (2011) applied a nanoindenter to measure mechanical properties of the wood-adhesive bond interphase within the cell wall, including hardness, elastic modulus, and deformation energy. For each specimen, 10 measurements were made along the interphase region with 5 µm spacing. This measurement method compared the mechanical properties of the wood-adhesive bond interphase with an instrument capable of nanoscale precision but provided limited information about the interactions taking place between the different phases of the interphase under load.

A more holistic approach accounting for interactions taking place throughout the volume of the interphase under load has been recently proposed by Kamke et al. (2014), who developed an integrated method for the quantitative assessment and numerical simulation of the elastic behavior of bonded wood systems. This method is capable of capturing the effects of adhesive penetration into cell lumens and the complex nature of the micromorphology of wood. This method coupled the numerical modeling of micromechanics of an adhesive bond interphase with microscale X-ray computed tomography (XCT) and optical measurements using the DIC principle. The purpose of the model based on the material point method (MPM) was to simulate the internal stress and strain distributions of the wood-adhesive bond interphase for the analysis of a number of manufacturing parameters (e.g., adhesive penetration). This model required a set of reliable morphological information as well as empirical data collected on a relevant scale for validation, optimization, and refinement (Muszynski et al. 2013). The 3D XCT digital tomograms at micron resolution facilitated phase differentiation within the interphase, including wood cells, adhesive, and void space (Paris et al. 2014). These morphology data were then directly used as a geometric input for a numerical model.

The aim of this paper is to describe the empirical methodology for the routine measurement of full-field deformations across adhesive bond interfaces in heterogeneous solids that constituted the third element of the integrated method and was developed in a parallel study. The specific objective of this study was to develop a methodology for the measurement and assessment of full-field elastic deformation and strain distributions across loaded wood-adhesive bond interphases of small lap shear specimens at a micromechanical level. This approach is a crucial element of the integrated inverse problem methodology as proposed by Kamke et al. (2014). A schematic diagram in Figure 1b illustrates this. The new approach was needed to obtain data for the validation, optimization, and refinement of a numerical model.

The intention of this paper is to present the methodological aspects of the study, and only sample results are needed for the illustration of the process. Full experimental results and the validation of the model will be presented in a separate publication.

Materials and methods

Introduction to the approach

It is important to stress that one of the basic premises of the project described in the introduction (Muszynski et al. 2013; Kamke et al. 2014) is a parallel development of the three aspects of the integrated method, and the works are developed in close collaboration to ensure full compatibility. Consequently, some aspects of the presented data below have to be seen in the context of the parallel studies and will be explained in reference to these studies.

Materials

The wood species and adhesive systems observed in this study were also used in the parallel study by Paris et al. (2014), aiming at the morphological definition of the bond interphase by means of X-ray microtomography. The wood species were Douglas fir [*Pseudotsuga menziesii* (Mirb.) Franco], loblolly pine [*Pinus taeda* (L.)], and hybrid poplar [*Populus trichocarpa* (Torr. & A. Gray)×*Populus deltoides* (W. Bartram ex Humphry Marshall)]. The adhesive systems were phenol-formaldehyde (PF), polymeric methylene diphenyl diisocyanate (pMDI), and poly(vinyl acetate) (PVAc). The adhesives were prepared with a contrasting agent to improve the X-ray attenuation of the XCT scans.

The specimens of approximately 2×2×15 mm^3 (R×T×L) were cut from two-layer laminates in six replicates of each of the selected wood species/adhesive combinations (a total of 54 specimens). Next,

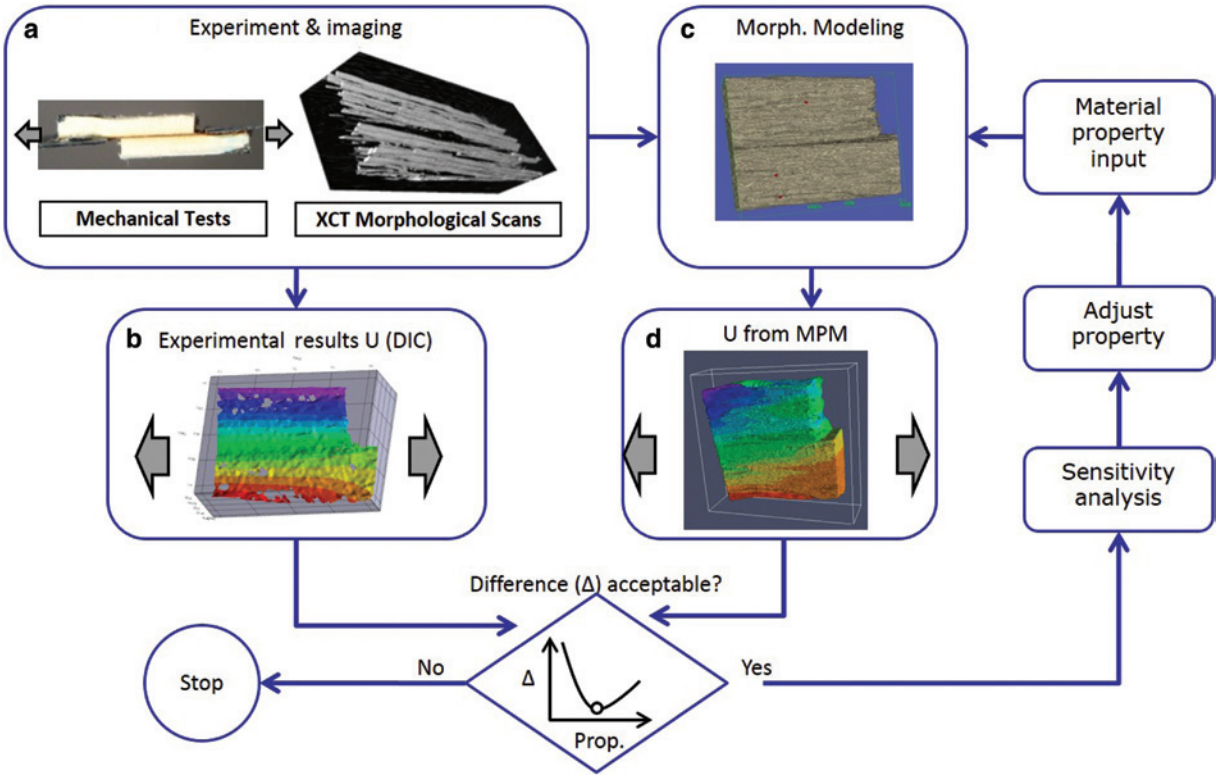

Figure 1 Diagram summarizing the data flow in the inverse problem approach as implemented in this project (Muszynski et al. 2013).

one R-L-plane of each specimen was microtomed to create a flat surface for optical measurements. Finally, a notch was created on each side by removing material with a small file and a razor blade to prepare the specimens for the microlap shear tests (Figure 2b).

Methods

At this stage, XCT scans were completed on all of the specimens to record the morphological structure of the bond interphases (Paris et al. 2014). To achieve micron-level resolution in the scan data, the total specimen scan volume was limited to 26.2 mm^3, which defined the lap shear specimen size. Following the scanning procedure, epoxy-graphite gripping tabs were glued onto the end arms of the specimen with a cyanoacrylate adhesive (Maximum Bond Krazy Glue® Gel, Westerville, OH, USA). All extension tabs were attached with the same glue type because the lap shear specimens were too small for direct mounting in the grips of the small universal machine.

An Instron ElectroPlus E1000 test machine (Instron, Norwood, MA, USA) was used for lap shear tests. The specimens were clamped in place by gripping the attached epoxy-graphite tabs (Figure 2b) in a way that ensured axial loading. The specimens were loaded in displacement control mode at a rate of 0.16 mm min^{-1} (strain rate, 0.014 mm min^{-1}) for 1 min. The total displacement was chosen, which did not break the specimens. The force was measured with an Instron 2518-807 load cell (±0.02 N) (Instron, Norwood, MA, USA). The force and displacement of the cross-head were recorded throughout the test. An analog force and position signal was recorded with a data acquisition unit. A nominal average shear stress over the bond plane served as a reference for the strain analysis.

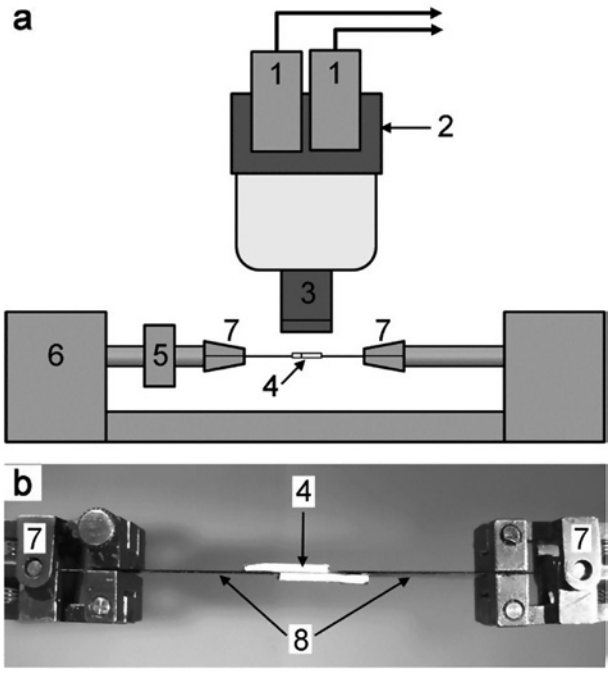

Figure 2 (a) Universal test machine showing lap shear specimen and DIC optical measurement system and (b) example of a lap shear specimen with ends bonded to graphite-epoxy tabs for attachment to test machine.
1, cameras; 2, beam splitter; 3, microscope objective; 4, specimen; 5, load cell; 6, test frame; 7, grip; 8, graphite-epoxy tab.

The displacements and strains on the surface were measured with an optical measurement unit (VIC-Micro 3D™, Correlated Solutions, Inc., Columbia, SC, USA) based on the DIC principle. The basic hardware components for this system consisted of two cameras, a stereomicroscope, and a beam splitter used to split the stereomicroscopic light path into two separate images. The two cameras were synchronized to assure that the two images were acquired at the same time. The system traces the displacements of a mesh of unique targets identified on the specimen surface. The small scale of the specimens required very fine random speckle patterns. Following the examples from other projects (Choi et al. 1991; Zink et al. 1995; Schwarzkopf and Muszyński 2014), these target patterns were created using printer toner powder. A uniform toner pattern was transferred onto the specimens by means of a custom-made air deposition apparatus (Schwarzkopf and Muszyński 2014) and fixed on the surfaces by heating in an oven at 103°C for 10 min. This temperature was much lower than the curing temperature of PF and pMDI adhesives used to form the bonds; therefore, no substantial degradation of wood polymer structure occurred. The moisture content of the specimens was below 9%. Given the small size of the specimens, no damage due to differential drying and warping was expected and none was observed.

During the test, the images of the specimen surface showing the bondline (field of view, 3.10×2.59 mm) were recorded every second for 1 min (60 images for every test) by means of the optical measurement system (Figure 2a). The boundaries of the XCT data (Figure 3b) defined the selected area of interest (AOI) for the optical measurement. For each individual test, the AOI was selected manually to ensure that the notch area scanned with XCT is included. The digital images, however, covered a larger area than the XCT scans.

The image sequences of the tests were processed by the dedicated analytical software VIC-3D 2010 (Correlated Solutions, Inc., Columbia, SC, USA) to calculate the surface coordinates, components of displacement vectors, and surface strain tensors. The size of the targets used for the DIC analysis (subset size) was 49 pixels, and the distance between the adjacent targets (step size) was 5 pixels. Using overlapping targets is a common method to generate a dense mesh of measurement points.

The accuracy and precision of optical measurements depend on the resolution of the camera and the intrinsic robustness of the DIC algorithm. Moreover, the quality of optics, lighting, focus, speckle pattern, selection of the algorithm options, and other parameters influence the results. The separate analysis of all impacts is tedious and impractical. Instead, the accuracy and precision of the system is assessed by a statistical analysis of a series of displacement and strain maps recorded on undeformed specimens. The expected mean displacements and strains in all directions are zero, so all recorded nonzero values can be thought of as the noise of the optical measurement system. The mean displacement and strains recorded for all data points within the AOI provides a convenient measure of accuracy, whereas the SD of the recorded noise provides a measure of the system's precision. These values may be different for each specimen due to different speckle patterns and specimen morphology. As an example, the accuracy and precision of the optical measurements for the specimen illustrated in Figure 4 was 0.069±0.015 µm for displacements in the x-direction and 0.101±0.013 µm for displacements in the y-direction. The accuracy and precision for strains was 0.641±80.664 µm m^{-1} in the x-direction and 4.806±92.083 µm m^{-1} in the y-direction.

The numerical data output generated by the optical measurement system was compatible with the numerical output of the MPM morphology-based modeling for test simulation (Kamke et al. 2014). Although this step is not necessary for quantitative analysis, both outputs can be presented in the form of color-coded maps of strains and displacements overlaid on the deformed specimen image. These maps allow a quick visual inspection of strain distribution, identification of potential stress concentrations, and interactions between components. The surface strains measured with the optical system provide unique "fingerprints" of the specimens, which are suitable for the validation of the numerical model (Muszynski et al. 2013; Nairn et al. 2013; Kamke et al. 2014).

The analysis of the efficiency of load transfer across the bond interphase was performed on 3D stress data generated by the validated numerical model. However, the principle of the analysis may be prototyped and illustrated on the surface strain data obtained

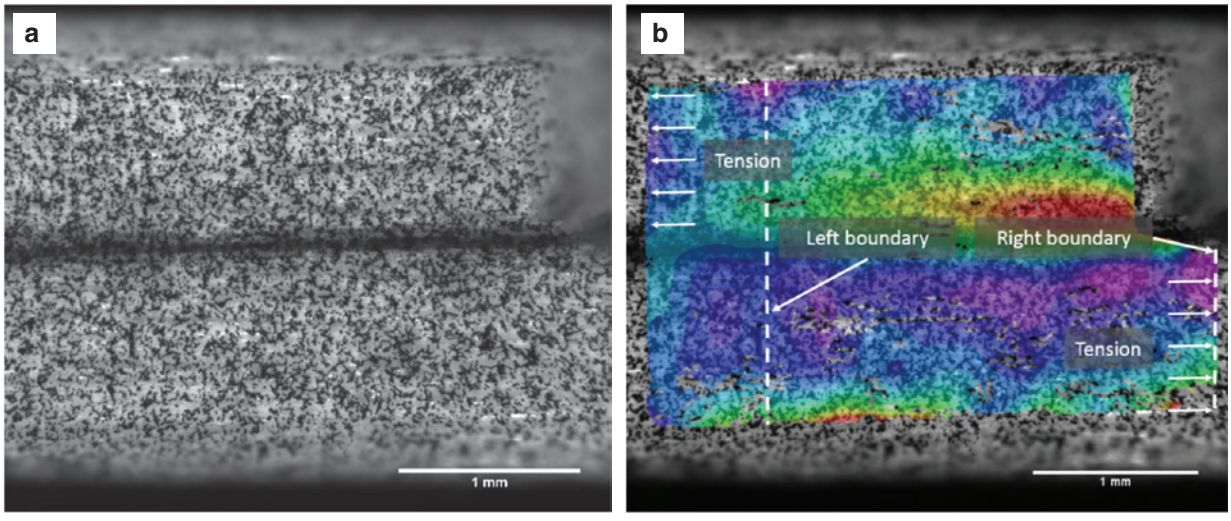

Figure 3 (a) Lap shear specimen with toner particle speckle pattern applied and (b) lap shear specimen with shear strain plot overlaid on the surface.
The left and right boundaries of the XCT scanned data are marked with dotted lines.

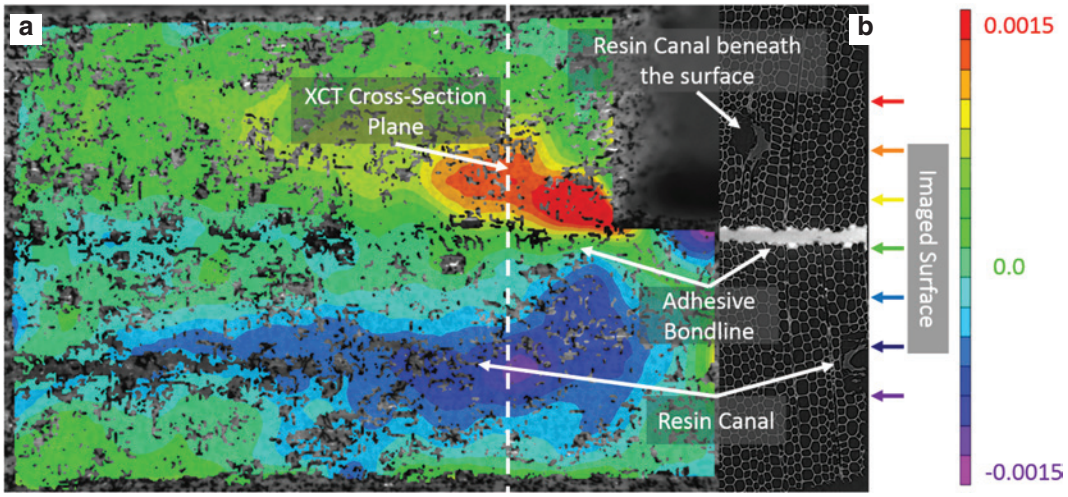

Figure 4 (a) Measured shear strain of a Douglas fir specimen with a PVAc-type adhesive and (b) XCT scan of the same specimen.

from the optical measurements, although the surface data may not be representative of the entire volume.

The analysis is based on the observation that the probability of a local failure event is correlated to the occurrence and accumulation of microflaws and resulting areas with high stress or strain concentrations (Weibull 1939) that may (but do not have to) initiate failure of the wood-adhesive bond. The probability of failure increases with the number and extent of the areas or volumes subjected to excessive stress or strain levels. If it is true that an efficient load transfer should not trigger premature failure of the bond, a statistical analysis of the full-field and volumetric stress and/or strain fields may provide a quantitative measure of such defined bond efficiency. One of the simplest approaches would be a number of measurement points characterized by stress or strain value above a certain arbitrary selected limit value. For data sets with regular spacing of points, for which the strains are measured or stresses are calculated, this number will represent the total volume subjected to excessive stress or strain. When normalized by the total volume/AOI (total number of measurement points), such a parameter may then serve as a quantitative characteristic of the efficiency of load transfer through the adhesive bond in question (smaller numbers indicating more efficient load transfer) and can be used for the assessment and comparison of various adhesive systems or combinations of bonding parameters.

Results and discussion

In Figure 5, a shear strain map measured on a physical specimen was compared with a simulated strain field obtained by a simplified finite element analysis (FEA) model. In this simplified approach, only the 2D contour of the lap shear was considered and the specimen was assumed to be a continuous solid. This comparison provided a quick qualitative check but was not suited for quantitative analysis. A strain concentration was seen near the notch area, where the load of one laminate was expected to be transferred to the other. This was in agreement with the observations by Müller et al. (2005)

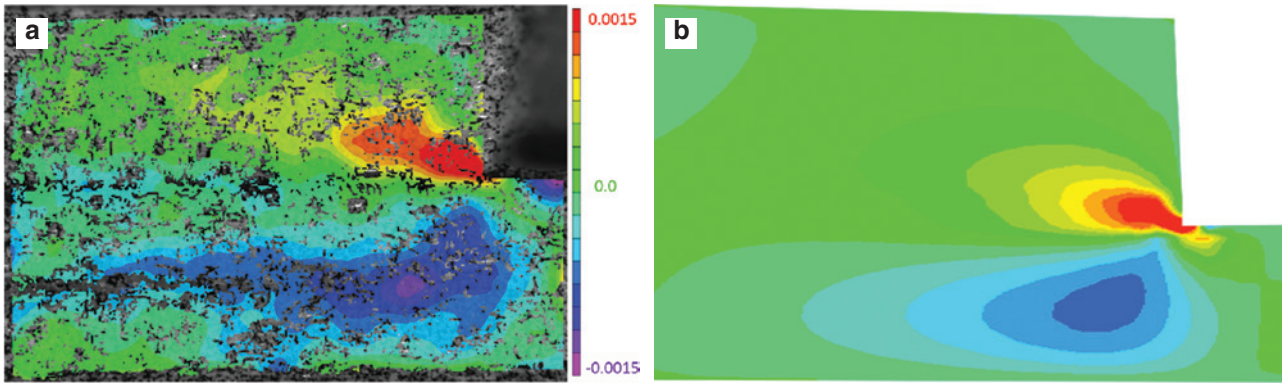

Figure 5 (a) Optical measurement of shear strains and (b) simplified FEA simulation of shear strain produced by Nairn et al. (2013).

and Serrano and Enquist (2005). The visual agreement between the two images added confidence to the simulation of stress and strain development in the complex interphase system. As already stated, the numerical output of the optical measurements can be directly compared with the numerical output of the numerical simulation to help verify and refine the 3D morphology-based MPM numerical model (Muszynski et al. 2013; Nairn et al. 2013; Kamke et al. 2014). This aspect, however, will be covered in a separate publication.

Compared with the simplified FEA simulation, the strain maps of the observed physical specimens were less regular and characterized by substantial variability resulting from anatomical features on or below the surface. These features can be investigated in the XCT scan data generated for the same specimen. For example, a Douglas fir specimen with a PVAc-type adhesive (Figure 4) showed a shear strain concentration (purple) in the lower laminate. This strain concentration seemed to be connected with a resin canal exposed on the surface. The resin canal was more compliant than the surrounding tracheids and deformed more easily. The XCT scan also revealed a second resin canal in the upper laminate beneath the surface. Figure 6 shows a different Douglas fir specimen also with a PVAc-type adhesive. This specimen also showed a high shear strain concentration (purple) on the surface of the lower laminate. A cross-section of the XCT scan of this specimen revealed that the lower laminate in the composite was composed of earlywood tracheid cells. Such cells were larger in diameter and had thinner cell walls and were consequently more compliant to angular deformations than the thick-walled latewood cells seen in the upper laminate. This kind of morphologic feature would be missed and would likely confuse the analysis if the surface strains would be considered to be representative of the entire specimen volume. Due to this morphological heterogeneity between specimens, qualitative assessments of surface strain patterns alone had a limited value. The variability, however, was of great value for the assessment of the accuracy and ultimate validation of the morphologically accurate model. The unique strain patterns affected by local anatomical features provided "fingerprints" of individual specimens.

As explained in the previous section, the measured surface strain data was also used for the prototyping and demonstration of the potential analysis of the efficiency of load transfer across the bond interphase. Figure 7 illustrates six shear strain maps for Douglas fir specimens with a PVAc-type adhesive. For each specimen, a histogram was generated representing the probability of measurement points within certain shear strain values. If the probability of premature specimen failure increases with the increasing area or volume subjected to extreme shear strain levels, then a count of the related data points could serve as a crude quantitative characteristic of the efficiency of load transfer through the bond. Based on an arbitrarily chosen shear strain cutoff level of ±0.002, the number of points above or below this range is displayed in Figure 7 between the color maps and histograms. In this comparison, specimen 2 had the most points (10,241 points) above or below this threshold and specimen 4 has the least (0 points). Based on this analysis, specimen 4 has the most efficient bond. As discussed above, one limitation of DIC analysis is that the strains are measured only on the surface of the specimen, which is hardly representative of the strain state in other positions throughout the depth of the specimen. For a more reliable analysis of bond efficiency, one would need to include the strain and

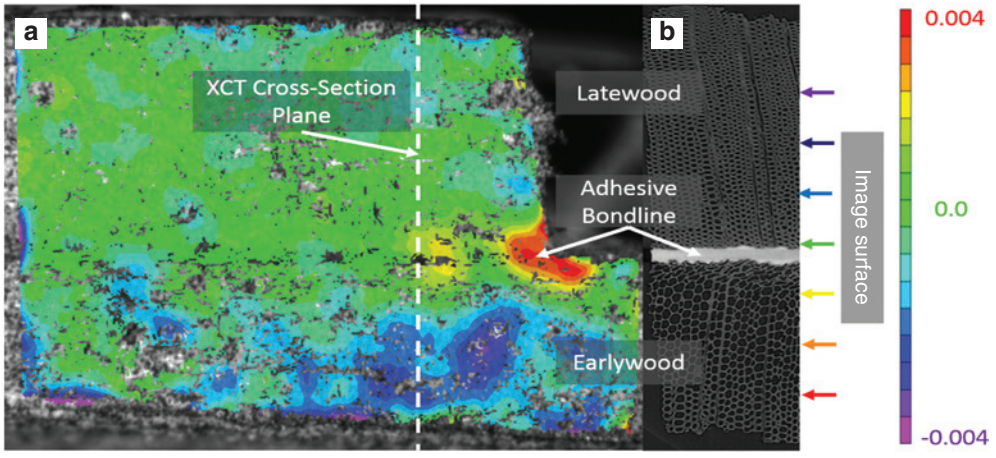

Figure 6 (a) Measured shear strain of a Douglas fir specimen with a PVAc-type adhesive and (b) XCT scan of the same specimen.

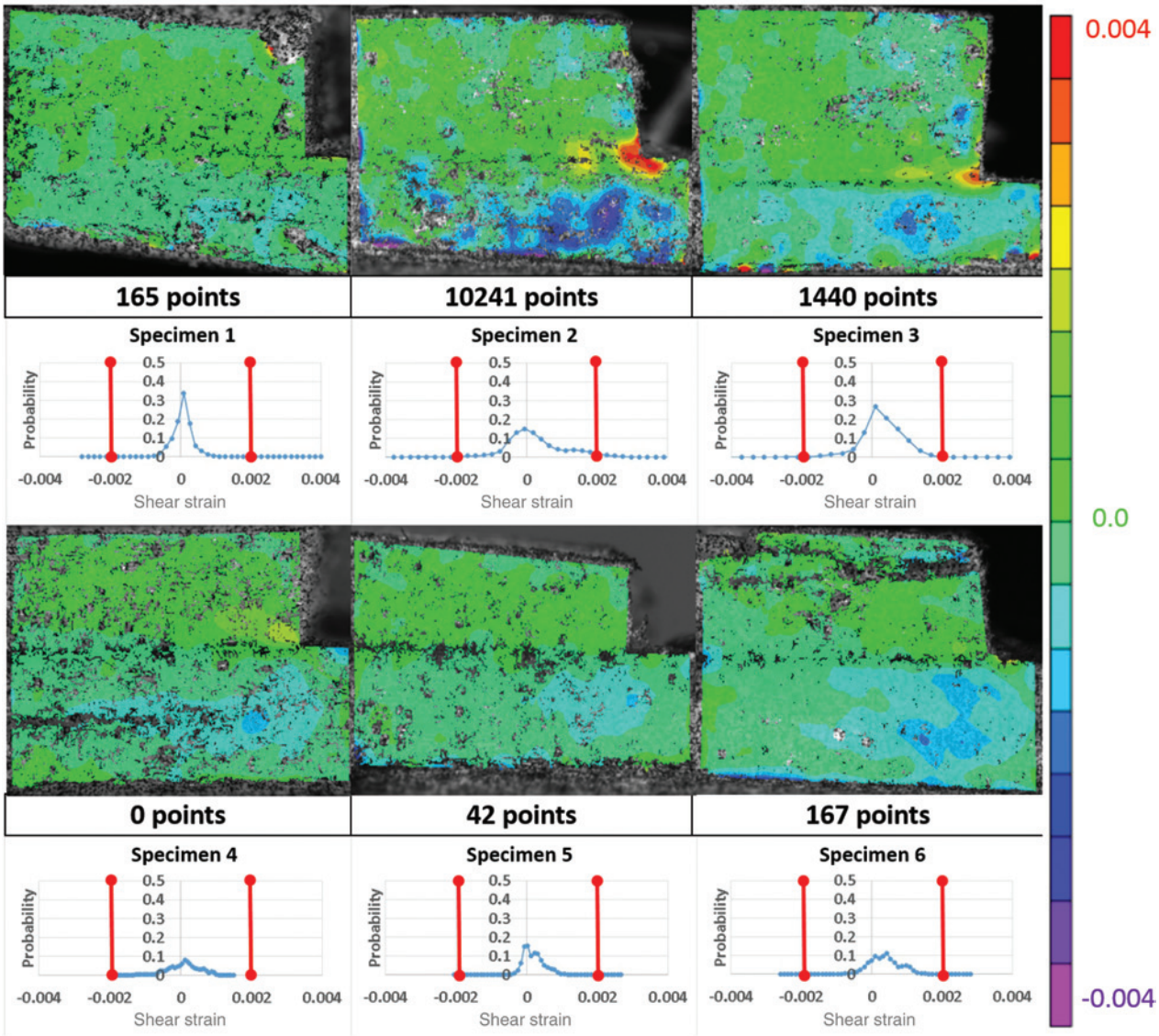

Figure 7 Shear strain plots overlaid on deformed specimen images compared with histograms showing the distribution of pixels strained to different levels.
Red markers signify the ±0.002 threshold. The total number of points outside this range is shown below the strain maps. All specimens are Douglas fir with a PVAc-type adhesive and are compared at a nominal stress of 5 MPa.

stress analysis of the entire volume of the specimen. This can only be obtained from the numerical simulation of the test in 3D and is the ultimate application of the full-field data obtained by means of this methodology.

Conclusions

A methodology is presented for measuring and assessing the full-field deformation and strain distribution across the loaded wood-adhesive interphase at a micromechanical level. The measurement of surface displacements and strains was substantially affected by the local morphology unique to a specimen under examination. Although the local variations do not allow general conclusions regarding the efficiency of load transfer in analyzed specimens, they provide "fingerprints" of individual specimens needed for the efficient assessment, refinement, and validation of the numerical model. Simulated stress and strain data obtained from such validated model may then be used for the meaningful analysis of the efficiency of load transfer across the adhesive bond interphase at this scale.

Acknowledgments: This research project was funded by the Wood-Based Composites Center, a National Science Foundation Industry/University Cooperative Research Center (Award No. IIP-1034975). The authors would also like to acknowledge John Nairn for providing numerical modeling simulations.

References

ASTM D2339-98. Standard test method for strength properties of adhesives in two-ply wood construction in shear by tension loading. ASTM International, West Conshohocken, PA, 2011.

ASTM D905-08. Standard test method for strength properties of adhesive bonds in shear by compression loading. ASTM International, West Conshohocken, PA, 2013.

ASTM D906-98. Standard test method for strength properties of adhesives in plywood type construction in shear by tension loading. ASTM International, West Conshohocken, PA, 2011.

Choi, D., Thorpe, J.L., Hanna, R.B. (1991) Image analysis to measure strain in wood and paper. Wood Sci. Technol. 25: 251–262.

Clauß, S., Gabriel, J., Karbach, A., Matner, M., Niemz, P. (2011) Influence of the adhesive formulation on the mechanical properties and bonding performance of polyurethane prepolymers. Holzforschung 65:835.

Kamke, F.A., Lee, J.N. (2007) Adhesive penetration in wood – a review. Wood Fiber Sci. 39:205–220.

Kamke, F.A., Nairn, J.A., Muszynski, L., Paris, J.L., Schwarzkopf, M., Xiao, X. (2014) Methodology for micromechanical analysis of wood adhesive bonds using X-ray computed tomography and numerical modeling. Wood Fiber Sci. 46:15–28.

Müller, U., Sretenovic, A., Vincenti, A., Gindl, W. (2005) Direct measurement of strain distribution along a wood bond line. Part 1: shear strain concentration in a lap joint specimen by means of electronic speckle pattern interferometry. Holzforschung 59:300.

Muszynski, L., Kamke, F.A., Nairn, J.A., Schwarzkopf, M., Paris, J.L. (2013) Integrated method for multi-scale/multi-modal investigation of micro-mechanical wood-adhesive interaction. In: International Conference on Wood Adhesives, October 9–11, 2013, Toronto, Ontario, Canada. p. 17.

Nairn, J.A., Kamke, F.A., Muszynski, L., Paris, J.L., Schwarzkopf, M. (2013) Direct 3D numerical simulation of stresses and strains in wood adhesive bond lines based on actual specimen anatomy from X-ray tomography data. In: International Conference on Wood Adhesives, October 9–11, 2013, Toronto, Ontario, Canada. p. 11.

Paris, J.L., Kamke, F.A., Mbachu, R., Gibson, S.K. (2014) Phenol formaldehyde adhesives formulated for advanced X-ray imaging in wood-composite bondlines. J. Mater. Sci. 49:580–591.

Schwarzkopf, M., Muszyński, L. (2015) Strain distribution and load transfer in the polymer-wood particle bond in wood plastic composites. Holzforschung 69:53–60.

Serrano, E., Enquist, B. (2005) Contact-free measurement and nonlinear finite element analyses of strain distribution along wood adhesive bonds. Holzforschung 59:641.

Valla, A., Konnerth, J., Keunecke, D., Niemz, P., Müller, U., Gindl, W. (2011) Comparison of two optical methods for contactless, full field and highly sensitive in-plane deformation measurements using the example of plywood. Wood Sci. Technol. 45:755–765.

Weibull, W. (1939) The phenomenon of rupture in solids. Ingeniörs Vetenskaps Akademien-Handlingar, 1939, Generalstabens Litografiska Anstalts Förlag.

Zink, A.G., Davidson, R.W., Hanna, R.B. (1995) Strain measurement in wood using a digital image correlation technique. Wood Fiber Sci. 27: 346–359.